



OPEN ACCESS

EDITED BY

Antonello Merlino,
University of Naples Federico II, Italy

REVIEWED BY

Andrea Ilari,
National Research Council (CNR), Italy
Luigi Vitagliano,
National Research Council (CNR), Italy

*CORRESPONDENCE

Saverio Santi,
✉ saverio.santi@unipd.it

RECEIVED 31 October 2025

REVISED 07 January 2026

ACCEPTED 09 January 2026

PUBLISHED 30 January 2026

CITATION

Difino A, Biondi B, Bisello A, Cardena R,
Lastella L, Šimić M, Calderaro B, Formaggio F,
Rancan M and Santi S (2026) Redox potential
fine tuning of ferrocene-peptide conjugates.
Front. Chem. Biol. 5:1736812.
doi: 10.3389/fchbi.2026.1736812

COPYRIGHT

© 2026 Difino, Biondi, Bisello, Cardena, Lastella,
Šimić, Calderaro, Formaggio, Rancan and Santi.
This is an open-access article distributed under
the terms of the [Creative Commons Attribution
License \(CC BY\)](https://creativecommons.org/licenses/by/4.0/). The use, distribution or
reproduction in other forums is permitted,
provided the original author(s) and the copyright
owner(s) are credited and that the original
publication in this journal is cited, in accordance
with accepted academic practice. No use,
distribution or reproduction is permitted which
does not comply with these terms.

Redox potential fine tuning of ferrocene-peptide conjugates

Alessia Difino¹, Barbara Biondi², Annalisa Bisello¹,
Roberta Cardena¹, Luana Lastella², Marko Šimić¹,
Beatrice Calderaro¹, Fernando Formaggio^{1,2}, Marzio Rancan³
and Saverio Santi^{1*}

¹Department of Chemistry, University of Padova, Padova, Italy, ²Institute of Biomolecular Chemistry, Padova Unit, National Research Council (CNR), Padova, Italy, ³Institute of Condensed Matter Chemistry and Technologies for Energy (ICMATE), National Research Council (CNR), Padova, Italy

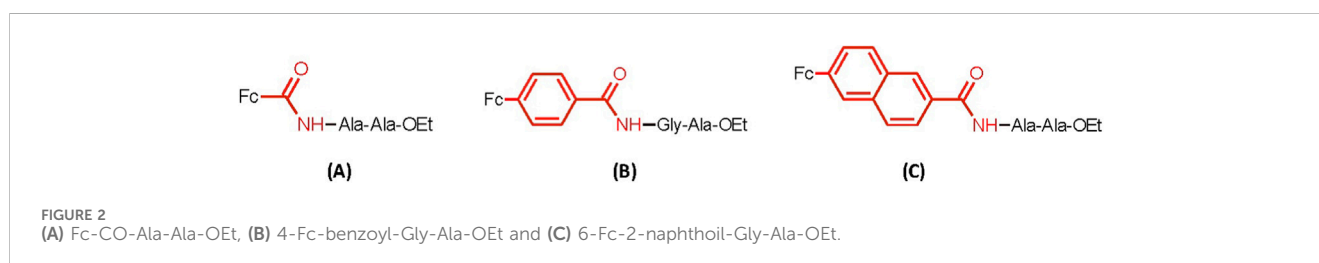
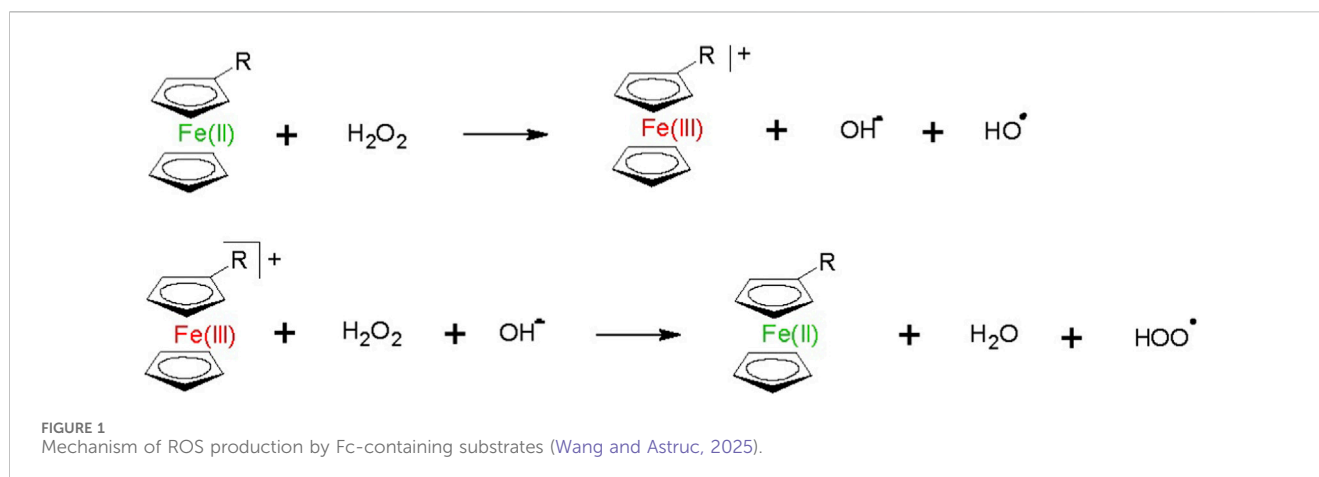
We report the synthesis of new ferrocene (Fc)-peptide conjugates, namely, N-Fc-succinamide-Gly-Ala-OEt, N-Fc-glutaramide-Gly-Ala-OEt, N-Fc-pimelamide-Gly-Ala-OEt, and N-Fc-glutaramide-Gly-Gly-Ala-OEt. They were designed on the base of four components: (i) a Fc unit as an electroactive element; (ii) the linker -NH-CO- to adjust the oxidation potential of Fc towards the physiological conditions; (iii) spacers of different lengths between Fc and the peptide; (iv) a peptide unit to drive Fc to selected biological targets. Fc-peptide conjugates have already been explored as potential anticancer drugs. It is reported that Fc displays the anti-proliferative activity through the production of reactive oxygen species (ROS) as its redox potential (0.40 V vs. SCE) is compatible with the intracellular potential which varies from +0.40 V to -0.44 V. However, the way Fc binds to the peptide significantly influences its redox potential. So far, this issue was not deeply addressed in the literature. Therefore, in this contribution we aimed at investigating the influence of the linker, and of the length of spacer and peptide on the Fc oxidation potential. Noteworthy, we linked Fc to the remaining part of the molecule via an amide bond, but with N-end attached to Fc and not the carbonyl, as reported in the literature so far. The cyclic voltammetry measurements we performed revealed that the transition from an electron-withdrawing (Fc-CO-NH-) to an electron-donating group (Fc-NH-CO-) significantly affects the Fc redox potential. On the contrary, spacer and peptide lengths display a moderate effect. We also carried out a conformational study in the crystal state (X-ray diffraction), and in solution (2D-NMR) on three intermediate molecules. Interestingly, the tripeptide Boc-Gly-Gly-Ala-OEt adopts a β -turn structure in all environments. This finding help to explain its resistance to the enzymatic hydrolysis. Enzymatic degradation tests in human serum were performed on the other conjugates as well, highlighting that the Fc unit acts as a protector of the peptide portion.

KEYWORDS

cyclic voltammetry, enzymatic degradation, ferrocene, peptide, X-ray structure

1 Introduction

Ferrocene derivatives have attracted considerable interest as anticancer, antibacterial, antifungal and antiparasitic drugs (Wang and Astruc, 2025; Ornelas and Astruc, 2023; Patra and Gasser, 2017; Gasser et al., 2011). In recent years we synthesized a variety of ferrocene-peptide conjugates with the aim at studying how the peptide skeleton affects charge and/or electron transfer. (Biondi et al., 2022; Bisello et al., 2023; Donoli et al., 2011; Santi et al., 2021;



Santi et al., 2022). In those studies, the ferrocene (Fc) unit was linked to the peptides *via* amide bond but in two different ways: N-linked, Fc-NH-CO-, or C-linked Fc-CO-NH. The different bonding mode resulted in an important decrease of Fc oxidation potential (of around 300–400 mV) from an electron-withdrawing group (-CO-NH-) to an electron-donating one (-NH-CO-).

Fc is a reliable and easy-to-handle electrochemical probe, but it is also able to promote the generation of reactive oxygen species (ROS) under physiological conditions. ROS concentrations higher than normal favor carcinogenesis, but at too elevated levels cytotoxic effects are observed. Indeed, literature reports refer of Fc-conjugates displaying anticancer activities (Ludwig, et al., 2021; Mooney et al., 2009; Zhou et al., 2012).

Recent studies have established that cellular uptake involves the internalization of ferrocene bound to transferrin, a plasma membrane transporter protein that mediates cellular iron uptake. This protein, as validated by a recent molecular docking study, can transport other metal ions or organometallic compounds from the bloodstream to all tissues. Furthermore, these studies have established that intrinsic apoptosis, also known as the mitochondrial pathway, is the primary mechanism driving ferrocene-triggered programmed cell death in tumor cells (Chaudhary et al., 2024). Furthermore ferroptosis, a different cell death pathway, is currently a subject of intense study for which it is well established that it involves iron-dependent lipid peroxidation and cell membrane damage (Meoli et al., 2025).

Tumor cells actively modify their metabolic pathways to meet their energy needs and maintain uncontrolled growth and proliferation. They display elevated levels of ROS due to oncogenic modification, which also leads to increased

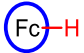
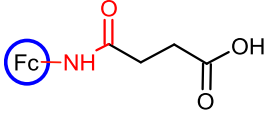
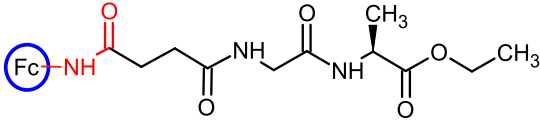
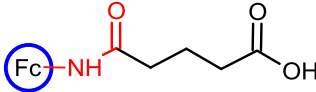
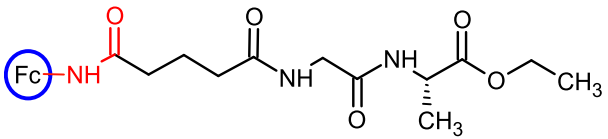
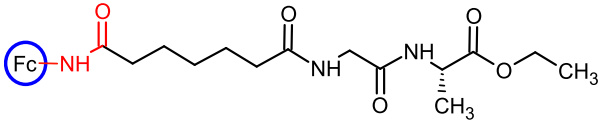
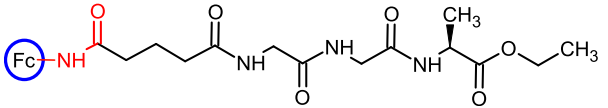
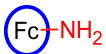
metabolism and mitochondrial dysfunction compared to healthy cells. Oncogenic cells are well-adapted to increase ROS levels by activating antioxidant pathways. However, ROS overload can cause negative consequences, including the oxidation of cell membranes, enzymes, or DNA, leading to cell death. Therefore, the increase of ROS concentration can be exploited as a cancer therapy. To this aim, two approaches can be envisaged: the first involves inhibiting the protective mechanisms developed by tumor cells, while the second involves the exogenous production of ROS, for example, through chemotherapy or radiotherapy.

The stress-induced damage of ferrocene activates an apoptotic signaling program that drives cell death, mediated by mitochondrial proteins, through the formation of pores on the outer mitochondrial membrane. However, higher levels of ROS can also trigger autophagy (Chaudhary et al., 2024). Therefore, apoptosis and autophagy play an essential role in the cell death cycle. Activating these mechanisms, however, requires an overload of ROS, which occurs because ferrocene and its derivatives can donate electrons to natural substrates, such as H₂O₂, a product of normal cellular metabolism, leading to the formation of highly toxic hydroxyl radicals (HO·) (Figure 1) (Wang and Astruc, 2025; Xu et al., 2022).

This property of Fc has been used to design various types of anticancer therapies. Early studies highlighted that a challenge to overcome for Fc application in medicine is its poor water solubility, being a particularly hydrophobic molecule.

It was shown that even if the lipophilic sandwich ligands allow the penetration through biological membranes, the water solubility is very important to the distribution of the drug into the organism (Neuse and Kanzawa, 1990). Both Fe(III) and Fe(II) derivatives could exhibit antitumor properties. Since Fc derivatives have long

TABLE 1 Compounds studied in this work.

ID	Compound	Molecular structure
Fc	Ferrocene	
1	N-Fc-succinic monoamide acid	
2	N-Fc-succinamide-Gly-Ala-OEt	
3	N-Fc-glutaric monoamide acid	
4	N-Fc-glutaramide-Gly-Ala-OEt	
5	N-Fc-pimelamide-Gly-Ala-OEt	
6	N-Fc-glutaramide-Gly-Gly-Ala-OEt	
Fc-NH ₂	Aminoferrocene	

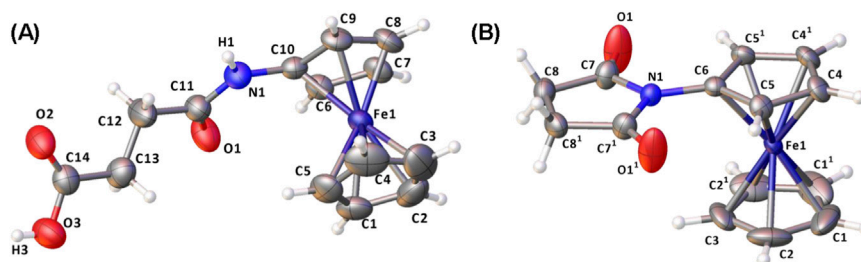


FIGURE 3
(A) Molecular structure of **1**. (B) Molecular structure of Fc-Su (symmetry operation: $1 = +x, 3/2-y, +z$). The thermal ellipsoids are drawn at the 50% probability level.

been known for their anticancer activities, the redox stability of both redox forms in biological media is a key aspect for their pharmacological applications. The lipophilic neutral Fe(II) form allows for transferring the derivative through biological membranes, whereas the cationic Fe(III) form provides solubility in hydrophilic media (Ornelas and Astruc, 2023).

Therefore, structures in which Fc is conjugated to a peptide that helps increase its solubility in the physiological environments have been studied for a long time (Ornelas, 2011).

Moreover, by exploiting electronic communication between organometallic fragments, it is possible to obtain optimized oligoferrocenes with redox potentials lower than those of the original ferrocenes. Fc cytotoxic activity is mediated by its ability to generate ROS as its redox potential (+0.4 V vs. SCE) is compatible with the intracellular values, which range from +0.40 V to -0.44 V vs. SCE (Kovacic et al., 1988; Kovacic, 2007).

However, the oxidation process is strongly influenced by the substituents attached to the cyclopentadienyl (Cp) rings, which modify their electronic distribution. For example, for the compound Fc-CO-Ala-Ala-OEt (Figure 2A) an E^0 value ($\approx E_{1/2}$) of 0.630 V vs. SCE is found, indicating that the presence of the dipeptide inhibits the oxidation of iron (Bauer et al., 1999).

This effect is due to the electron-withdrawing action of the carbonyl group, which depletes part of the electron density of Fc. Under these conditions, iron oxidation would lead to an additional positive charge that would add to the previous effect, making the complex more difficult to oxidize.

At variance, the oxidation potentials of 4-Fc-benzoyl-Gly-Ala-OEt (Harry et al., 2014) (Figure 2B) and 6-Fc-2-naphthoyl-Ala-Ala-OEt (Mooney et al., 2009) (Figure 2C) are significantly lower (0.473 and 0.442 V vs. SCE respectively), due to the presence of the aromatic spacers which distances Fc from the carbonyl group (reduced inductive effect) thus leaving a sufficient electron density on Fc. Therefore, Fc is more easily oxidized in a cellular environment. While the electron-withdrawing power of the carbonyl increases the oxidation potential, an aromatic moiety leaves it almost unaffected, in view of the extended conjugation of the π -electrons of the Cp rings that permits the oxidation of Fc under physiological conditions.

These considerations urged us to explore different conjugation moieties to Fc, in order to fine tuning its ability to promote ROS production in cells. Our aim was to favor electron-donating groups to maintain the redox potential at approximately +0.4 V (vs. SCE)

or, even better, to lower it. We then herein report synthesis, characterization, enzyme degradation assays and, most importantly, an in-depth cyclic voltammetry study of six new, Fc-conjugated molecules (Table 1), characterized by a Fc-N connections and by spacer and peptide units of different lengths.

2 Materials and methods

2.1 Peptide syntheses

Syntheses were carried out in an oxygen and moisture-free atmosphere. Solvents were dried by reflux over the appropriate drying agent and distilled under a stream of argon. Fc, Fc-NH₂, 1-hydroxy-benzotriazole hydrate (HOBt), diisopropylethylamine (DIEA), succinic anhydride, glutaric anhydride and pimelic acid were Sigma Aldrich products; 1-(3-dimethylaminopropyl)-3-ethylcarbodiimide (EDC), and L-alanine ethyl ester hydrochloride (H-L-Ala-OEt-HCl) were Iris Biotech products. Boc-Gly-L-Ala-OEt was prepared by literature procedures.

2.2 Mass spectrometry

MS spectra were obtained using an Agilent 6130 ESI-TOF mass spectrometer coupled to an HPLC system, collecting data in the positive mode. All compounds were analyzed by analytical HPLC and were >95% pure.

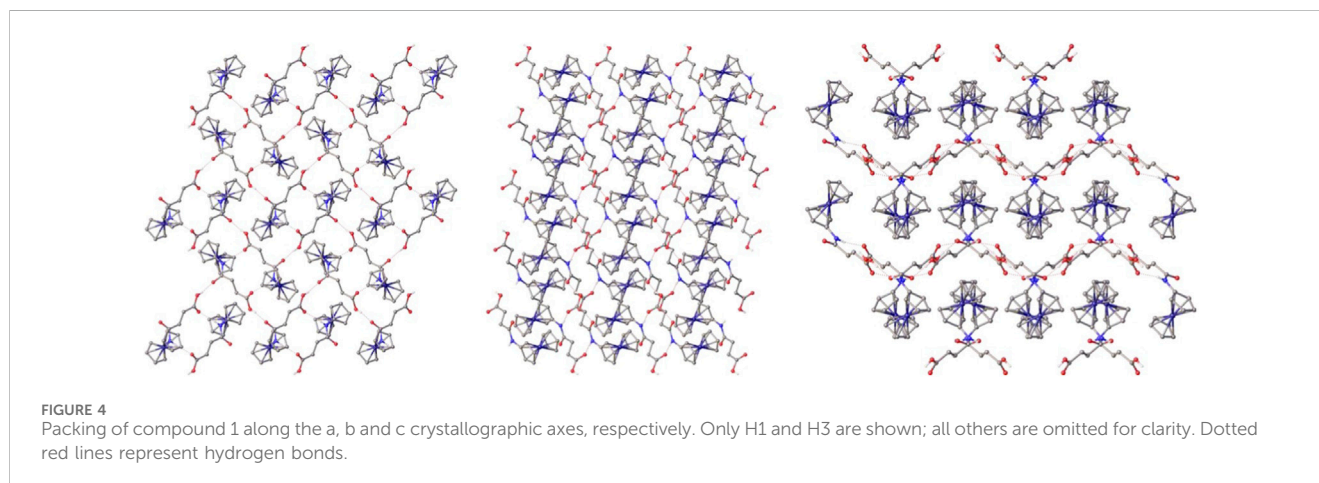
2.3 NMR spectra

Spectra were collected on a Bruker Avance III HD spectrometer operating at 400.13 MHz ($T = 298\text{K}$). The peptide concentration in solution was 1 mM in spectrograde CHCl₃-d₁ (99.8% D containing 0.5 %wt. of silver foils as stabilizers and 0.03% (v/v) tetramethylsilane-Eurisotop) and DMSO-d₆ (99.96% D-Eurisotop). Processing and evaluation of the experimental data were carried out using the TOPSPIN software packages. All homonuclear spectra were acquired by collecting 400 experiments, each consisting of 32 scans and 2K data points. The spin systems of the amino acid residues were identified using standard double-quantum filtered COSY (Rance et al., 1983) and

TABLE 2 Hydrogen bonds in **1**; D denotes the donor atom and A the acceptor atom.

D-H	d (D-H)/Å	d (H...A)/Å	<DHA/°	d (D...A)/Å	A
O3-H3	0.82	1.849	165.85	2.651	O1 [§]
N1-H1	0.86	2.079	167.68	2.925	O2 [#]

Symmetry operations: § = -x, y-1/2, -z+1/2, # = -x, -y+1, -z+1.



clean TOCSY (Griesinger et al., 1988) spectra. In the latter case, the spin-lock sequence was 70 ms long. NOESY experiments were utilized for sequence-specific assignments (Wüthrich, 1991; Boros et al., 2018).

2.4 X-ray diffraction

Data for **1** and N-ferrocenylsuccinimide (**Fc-Su**), obtained as byproduct in the synthesis of **2**, were collected using an Oxford Diffraction Gemini E diffractometer, equipped with a 2 K × 2 K EOS CCD area detector and sealed-tube Enhance (Cu-Kα, λ = 1.54178 Å) X-ray source. Data for compound **3** were collected on a Bruker D8 Venture diffractometer equipped with Incoatec IμS3.0 (EF) microfocus sealed-tube (Cu-Kα, λ = 1.54178 Å), a Montel layer optics monochromator, and a Photon III C14 CPAD area detector. Data reduction, finalization and cell refinement were carried out through the CrysAlisPro software. Empirical multi-scan absorption corrections using equivalent reflections have been performed with the scaling algorithm SCALE3 ABSPACK. Accurate unit cell parameters were obtained by least squares refinement of the angular settings of strongest reflections, chosen from the whole experiment. The structures were solved with Olex2 (Dolomanov et al., 2009) by using ShelXT structure solution program by Intrinsic Phasing and refined with the ShelXL refinement package using least-squares minimization (Sheldrick, 2015). In the last cycles of refinement, non-hydrogen atoms were refined anisotropically. Hydrogen atoms were included in calculated positions, and a riding model was used for their refinement. Supplementary Table S1 reports the crystal data and refinement details. Cambridge Crystallographic Data Centre (CCDC) numbers 2497229-2497,231 contain the supplementary crystallographic data for

this paper. These data are provided free of charge by the joint CCDC and Fachinformationszentrum Karlsruhe Access Structures service www.ccdc.ca-m.ac.uk/structures.

2.5 Cyclic voltammetry

The experiments were performed in an air-tight three-electrode cell connected to a vacuum/argon Schlenk line. Dichloromethane solvent was pre-dried with anhydrous calcium chloride, refluxed over calcium hydride and distilled under a stream of Argon. Solvent and *n*Bu₄NPF₆ were degassed in a Schlenk flask by manifold freeze-pump-thaw cycles and transferred by cannula in the cell. The reference electrode was a SCE (Tacussel ECS C10) separated from the solution by a bridge compartment filled with the same solvent/supporting electrolyte solution used in the cell. The counter electrode was a platinum spiral with around 1 cm² apparent surface area. The working electrode was a disk obtained from cross section of a gold wire with 0.5 and 0.125 mm diameter sealed in glass. Between successive scans, the working electrode was polished on alumina according to standard procedures and sonicated before use. An, E.G.,&G PAR-175 signal generator was used. The currents and potentials were recorded on a Lecroy 9310L oscilloscope. The potentiostat was home-built with a positive feedback loop for compensation of the ohmic drop (Amatore et al., 1989).

2.6 Peptide stability in serum

The peptides were dissolved in DMSO at a concentration of 5 mg/mL. In Eppendorf tubes, 1 mL of HEPES buffer (25 mM, pH = 7.6)

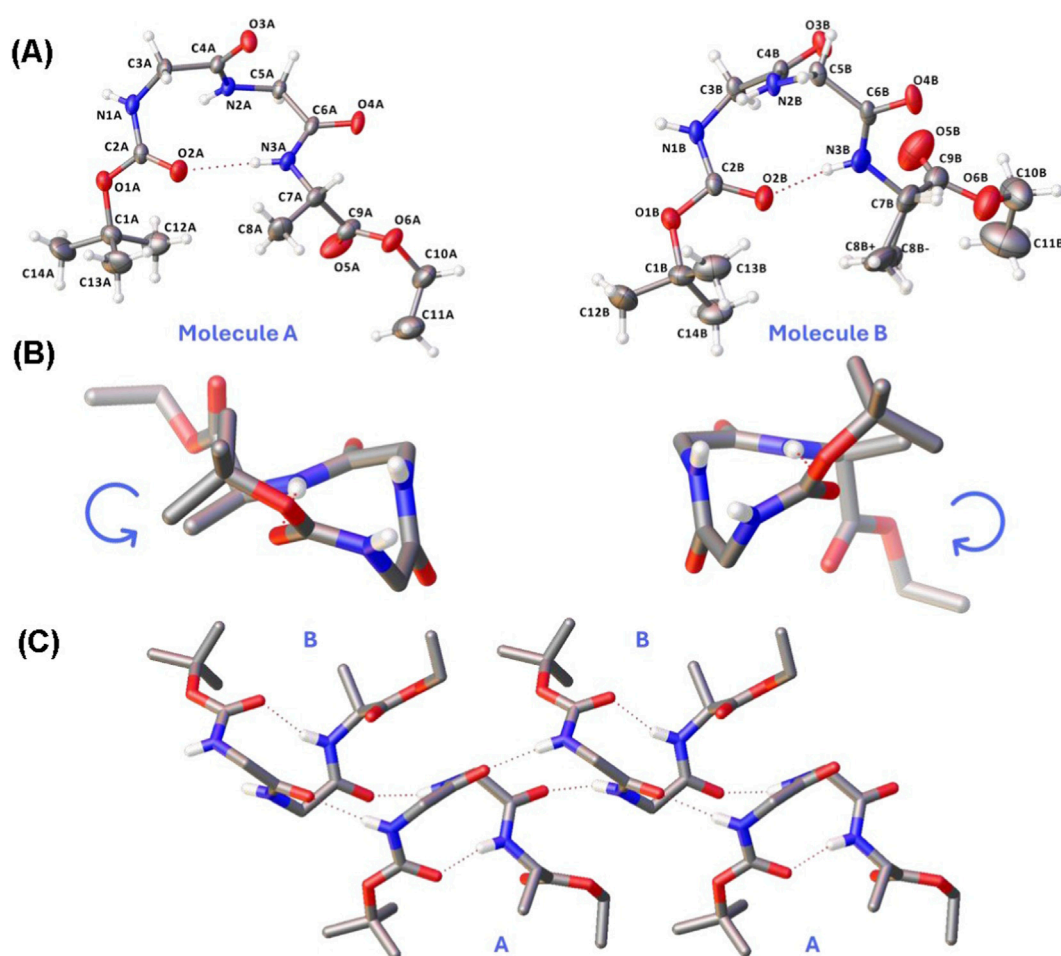


FIGURE 5
 (A) The two crystallographic independent molecules of Boc-Gly-Gly-Ala-OEt. (B) Opposite handedness of molecules A and B. (C) H-bond supported 1D chain of alternating molecules A and B. Dotted red lines represent H-bonds. The thermal ellipsoids are drawn at the 50% probability level.

was temperature equilibrated at 37 °C before adding 250 μL of human serum and 20 μL of peptide solution. The human serum used in these experiments was obtained from Merck. It is derived from platelet-poor human plasma. It is sterile-filtered and tested for viruses and *mycoplasma*. The reaction was monitored for 24 h. At fixed intervals, 100 μL of the solution was withdrawn and added with 200 μL of absolute ethanol. The sample was kept on ice for 15 min and then centrifuged at 16,000 g for 5 min. Finally, the supernatant solution was analyzed by HPLC or HPLC-MS. (Jenssen and Aspmo, 2008). A peptide of similar length, not resistant to degradation in serum, was used as a positive test. The peptide sequence is as follows: Tyr-Ser-Ser-Phe-Leu. To verify peptide stability in buffer solution, samples containing peptide solutions, buffer, and ethanol were also analyzed.

3 Results and discussion

3.1 Synthesis and structural determinations

Compounds 1-6 (Table 1) were synthesized by solution methods and characterized by HPLC-MS and NMR spectrometry as described

in detail in the Supplementary Material file. Briefly, peptide bonds were formed by activating the carboxylic function with the coupling reagents EDC/HOBt [EDC, N-ethyl-N'-dimethylaminopropylcarbodiimide; HOBt, 1-hydroxybenzotriazole]. HOBt suppresses racemization, when chiral amino acids are involved, but it also catalyzes the formation of amide bonds (Crisma et al., 1998). For this latter reason it was used even when chirality was not an issue. The amide bonds of compounds 1 and 3 were prepared by reacting Fc-NH₂ with succinic and glutaric anhydride, respectively. In the case of compound 5, Fc-NH₂ was first reacted with pimelic acid. The product obtained was isolated and, without further purification, reacted with H-Gly-Gly-Ala-OEt (see Supplementary Material).

When 1 was activated with EDC/HOBt to synthesize 2, we also obtained N-ferrocenylsuccinimide (Fc-Su) as a byproduct, due to an intramolecular amide (imide) bond formation (Supplementary Material). The same reaction occurred in the synthesis of 4, starting from 3, yielding a moderate amount of N-ferrocenylglutarimide (Supplementary Material). We were able to grow single crystals of both Fc-Su and its precursor, compound 1, and to determine their molecular structures by X-ray diffraction (Figure 3).

TABLE 3 Selected torsional angles in Boc-Gly-Gly-Ala-OEt.

Angle	Atom 1	Atom 2	Atom 3	Atom 4	Degree	Atom 1	Atom 2	Atom 3	Atom 4	Degree
ϕ_1	C2A	N1A	C3A	C4A	69.5°	C2B	N1B	C3B	C4B	-66.77°
ψ_1	N1A	C3A	C4A	N2A	10.5°	N1B	C3B	C4B	N2B	-15.45°
ϕ_2	C4A	N2A	C5A	C6A	72.4°	C4B	N2B	C5B	C6B	-71.76°
ψ_2	N2A	C5A	C6A	N3A	19.2°	N2B	C5B	C6B	N3B	-17.69°
ϕ_3	C6A	N3A	C7A	C9A	-64.1°	C6B	N3B	C7B	C9B	-87.51°
ψ_3	N3A	C7A	C9A	O6A	144.8°	N3B	C7B	C9B	O6B	162.94°

TABLE 4 Hydrogen bonds in Boc-Gly-Gly-Ala-OEt; D is the donor atom and A the acceptor atom.

D-H	d (D-H)/Å	d (H...A)/Å	<DHA/°	d (D...A)/Å	A
N2A-H2A	0.86	2.107	159.2	2.927	O4B
N1A-H1A	0.86	2.134	168.59	2.982	O3B
N3A-H3A	0.86	2.172	160.32	2.995	O2A
N1B-H1B	0.86	2.096	164.91	2.935	O3A [§]
N3B-H3B	0.86	2.207	154.39	3.006	O2B
N2B-H2B	0.86	2.122	161.37	2.95	O4A [§]

Symmetry operation: § = x-1, y, z.

The structure of **1** was solved in the monoclinic space group $P2_1/c$, while that of **Fc-Su** was solved in the monoclinic space group $P2_1/m$. In both structures, the cyclopentadienyl rings coordinate to the Fe(II) ion with η^5 hapticity, adopting a nearly eclipsed configuration. Such an arrangement has been previously observed in several ferrocene derivatives (Donoli et al., 2013; Santi et al., 2021; Biondi et al., 2021; Biondi et al., 2022). The Fe-C bond lengths range from 2.025 to 2.045 Å, while the distances between the Fe(II) ion and the centroids of the cyclopentadienyl rings are between 1.642-1.644 Å.

Interestingly, in **1** the angle between the plane of the cyclopentadienyl ring (C6-C10) and the plane defined by atoms N1-C11-O1-C12 is 8.3°, whereas in **Fc-Su**, the angle between the cyclopentadienyl plane (C4-C5-C6-C5'-C4') and the succinimide plane is only 0.2°. This coplanarity suggests that an extended π -conjugation is established between Cp and the imide of **Fc-Su**. Such conjugation exists also between Cp and the amide in **1**, although to a lower extent.

In compound **1**, the N1-H1 and O3-H3 groups participate in intermolecular hydrogen bonds with atoms O2 and O1, respectively, as described in Table 2 and shown in Figure 4.

We were also able to solve the crystal structure of Boc-Gly-Gly-Ala-OEt, the tripeptide intermediate used in the synthesis of compound **6**. The structure was determined in the monoclinic space group $P2_1$. The asymmetric unit comprises two crystallographic independent molecules, designated A and B (Figure 5A). Both molecules feature a $i \rightarrow i+3$ intramolecular C=O...H-N hydrogen bond, which stabilizes a β -turn conformation. In molecule A, the ϕ and ψ dihedral angles adopt values close to those characteristics of a type III' β -turn, whereas molecule B exhibits negative angles consistent with a type III β -turn

(Table 3) (Venkatachalam, 1968). The intramolecular hydrogen bond forms a 10-membered pseudo-cycle with very similar geometries in both molecules, with N...O donor-acceptor distances of approximately 3.0 Å for A (N3A...O2A) and B (N3B...O2B) (Table 4).

Intermolecular H-bonds connect molecules A and B into a 1D supramolecular chain, arranged in an alternating A-B sequence (Figure 5C). This motif is sustained by N1A...O3B and N2A...O4B H-bonds, along with the reciprocal N1B...O3A and N2B...O4A interactions (Table 4).

This β -turn structure was rather unexpected, as Gly usually prefers to adopt extended conformations. We may argue that the β -turn was promoted by the crystal packing and/or by the achiral nature of Gly. Indeed, the two independent molecules exhibit opposite helical handedness and form a pseudo-racemate: molecule A twists anticlockwise and molecule B clockwise (Figure 5B). It is well known that racemates and pseudo-racemates crystallize easily and facilitate structure resolution (Zawadke and Berg, 1993; Doi et al., 1993; Toniolo et al., 1994). However, we are inclined to believe that the observed bended conformation of Boc-Gly-Gly-Ala-OEt does not depend on packing or chirality because it is maintained in solution and also when the tripeptide is linked to Fc. As a matter of fact, typical cross-peaks of turn/helical peptide conformations (Wüthrich, 1991) are observed in the NOESY spectrum of **6** in CDCl₃ solution. Both $NH_i \rightarrow NH_{i+1}$ connectivities characterizing the β -turn are clearly detected (Figure 6). Since the β -turn involves the two achiral Gly residues, the left- and right-turn form likewise with the same probability. However, we are unable to assess if one conformation prevails over the other because they interconvert at a much faster rate than the NMR time scale (Hummel et al., 1987).

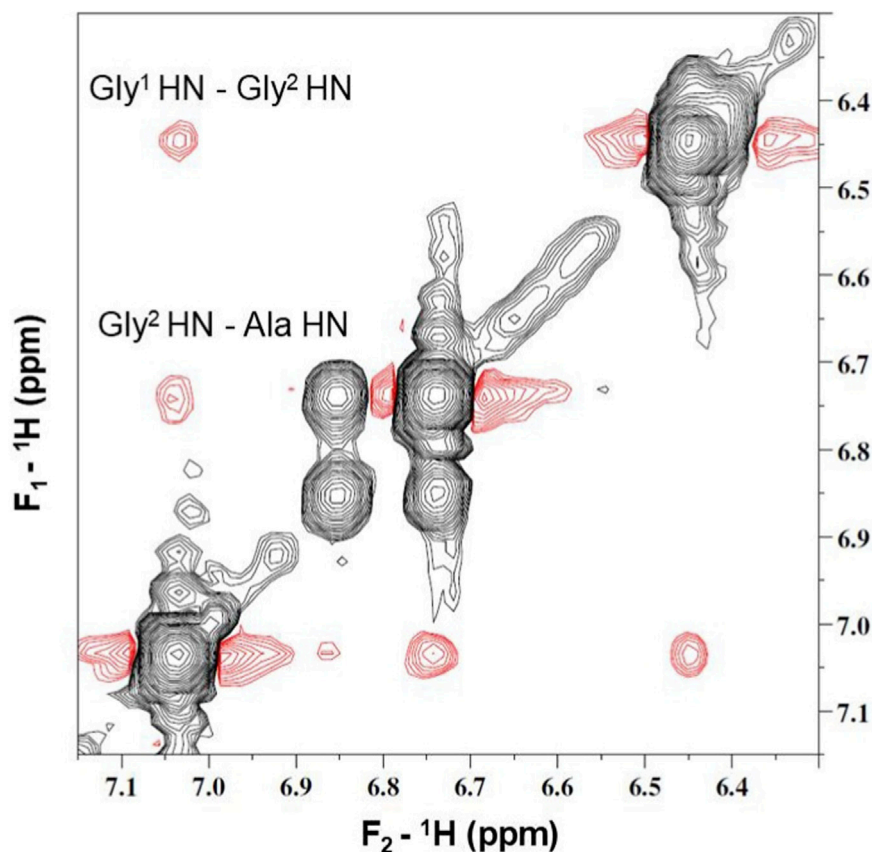


FIGURE 6
Section of the NOESY spectrum of **6** at 1 mM concentration in CDCl₃ solution.

Moreover, the stable presence in solution of such β -turn could account for the fair resistance to enzymatic degradation of compound **6** (see below).

3.2 Cyclic voltammetry analysis

Fc is a very useful redox probe as it is stable in water, it is insensitive to air in both neutral and oxidized states, it is soluble in common organic solvents and in addition it displays a low oxidation potential. As previously pointed out, the way Fc binds to an organic moiety significantly influences its redox potential. To better understand this issue, we prepared the above-mentioned Fc-conjugates, that differ for spacer and peptide length, but share the way Fc is connected, *i.e.*, the amide nitrogen (Fc-NH-CO-). The most exploited way to conjugate Fc to a peptide for creating new drugs has been so far Fc-CO-NH-. With our new molecules, we expect to lower the Fc redox potentials below the original ferrocene values, and thus make them compatible with the intracellular redox potentials, which range from +0.40 V to -0.44 V vs. SCE.

The cyclic voltammograms of the peptides N-Fc-succinamide-Gly-Ala-OEt (**2**), N-Fc-glutaramide-Gly-Ala-OEt (**4**), N-Fc-pimelamide-Gly-Ala-OEt (**5**), N-Fc-glutaramide-Gly-Gly-Ala-OEt (**6**), and of the carboxylic acids Fc (**1**) and Fc-NH₂ (**3**) are reported in Figure 7. All measurements were performed in

dichloromethane solution in the presence of (nBu)₄BPF₆ (0.1 M) as a supporting electrolyte.

The main objective was to evaluate the effect exerted on the oxidation potential ($E_{1/2}$) by the -NHCO- group, the spacer and the peptide and consequently to assess the suitability of these compounds to meet the intracellular redox conditions. The electron-donating properties of the -NHCO- group determine a decrease of the oxidation potential of Fc down to 0.3 V for some of our molecules (Table 5). On the contrary, the electron-withdrawing effect of the -CONH- group causes an increase in the oxidation potential up to values of 0.6–0.8 V (see, for example, Biondi et al., 2022), which are not compatible with the intracellular environment (between 0.40 and -0.44 V vs. SCE).

It can be observed that all the products analyzed show a single, reversible, Nernstian monoelectronic oxidation wave ($\Delta E_p = 60$ –70 mV, Table 5) in the scan rate ν range between 0.1 and 5 Vs⁻¹, on electrode gold disc working with diameter $d = 0.125$ mm (0.5–5 Vs⁻¹) and 0.5 mm (0.1–0.5 Vs⁻¹).

As expected, the $E_{1/2}$ values demonstrate that the Fc-NH-CO-linkage, *i.e.*, Fc directly connected to N, has the major effect on the oxidation potential of our Fc-peptides, anticipating by 100–120 mV with respect to Fc, with the greatest decrease obtained for peptide **5**. Apparently, a long spacer helps decrease the $E_{1/2}$ values, probably because it moves far apart the second, electron-withdrawing carbonyl. This conclusion agrees with the behavior of **1** and **3**, as

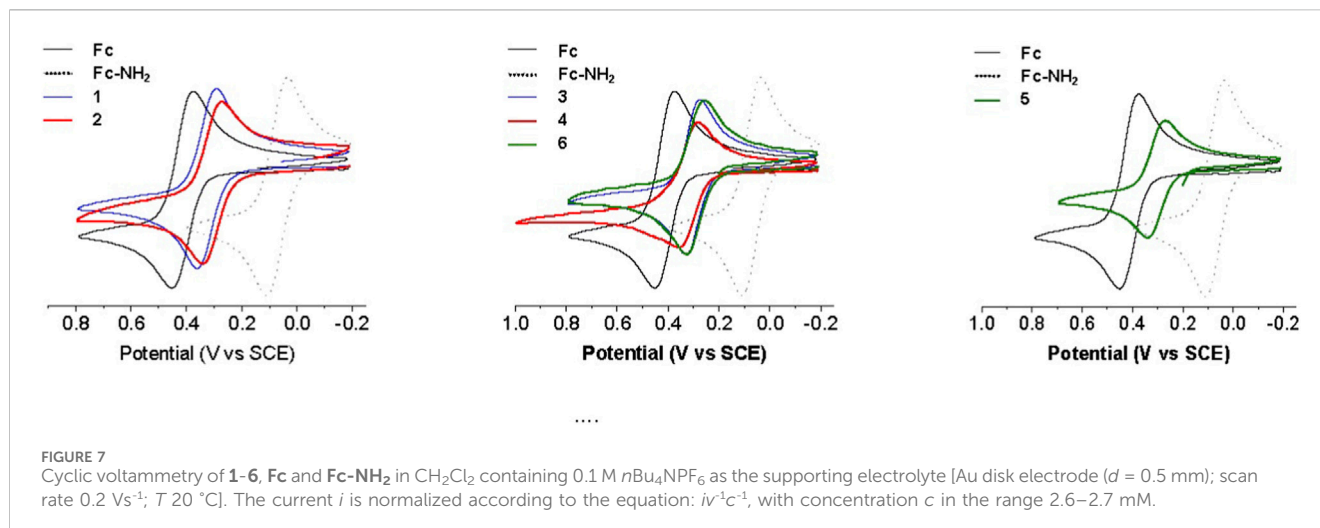


TABLE 5 Electrochemical data: E_p = peak potential (anodic), $E_{p/2}$ = potential at $i = i_{p/2}$, $E_{1/2} = E_{p/2} + \Delta E_p/2$ half-wave potential, $\Delta E_p = E_p - E_{p/2}$, $\delta E = \pm 2$ mV. Potential scanning speed $\nu = 0.2$ Vs⁻¹. The current is normalized according to the equation $i\nu^{-1/2}c^{-1}$.

ID	Compound	E_p (V)	$E_{p/2}$ (V)	$E_{1/2}$ (V)	ΔE_p (mV)
Fc	Ferrocene	0.45	0.39	0.42	60
1	N-Fc-succinic monoamide acid	0.36	0.30	0.33	60
2	N-Fc-succinamide-Gly-Ala-OEt	0.34	0.28	0.31	60
3	N-Fc-glutaric monoamide acid	0.33	0.27	0.30	60
4	N-Fc-glutaramide-Gly-Ala-OEt	0.35	0.29	0.32	70
5	N-Fc-pimelamide-Gly-Ala-OEt	0.33	0.27	0.30	60
6	N-Fc-glutaramide-Gly-Gly-Ala-OEt	0.34	0.28	0.31	60
Fc-NH ₂	Aminoferrocene	0.11	0.05	0.08	60

the latter endowed with a longer chain displays a 30 mV reduction of $E_{1/2}$.

The length of the peptides also appears to have an effect, albeit a moderate one. The $E_{1/2}$ value of **6**, containing a tripeptide, is slightly lower than in the case of **4**, a conjugate with a dipeptide.

Overall, all Fc-peptides (**2** and **4-6**) have shown to possess redox values compatible with the intracellular potentials.

3.3 Peptide enzymatic degradation

The stability of Fc-peptide conjugates against proteolytic degradation is a major challenge in their development as potential anticancer agents. In this study, we investigated the stability of the synthetic peptides when exposed to human serum. After incubation with serum, the integrity of the conjugates was monitored by HPLC. Proteolytic degradation is reported as a function of time (Peggion et al., 2025; Albini, et al., 2025).

Considering the dipeptide Gly-Ala conjugated to Fc via linkers of different lengths, we observed rapid degradation of **4**, whereas **2** exhibited a slower degradation rate (Figure 8). We concluded that the Fc moiety exerts a protective effect on the Gly-

Ala sequence, depending on the distance between the Fc moiety and the peptide.

Surprisingly, a notably different pattern of degradation was observed for **6**. Here, the peptide moiety is represented by the Gly-Gly-Ala sequence, and the Fc unit is connected to the peptide via the same linker as in compound **4**. In this case, the percentage of intact peptide was around 60% after 3 h, and almost 30% of the peptide was still present after 24 h (data not shown). The conformational analysis conducted on the free peptide and on **6** revealed the presence of a β -turn structure. This structural feature led us to interpret the observed resistance to proteolysis as an effect of conformational stability rather than the protective role of the Fc moiety.

4 Structure-property relationships

The most important structural feature of our new Fc-peptides is the presence of the Fc-NH-CO- moiety, whereas the most exploited way of connection has been so far Fc-CO-NH-. Indeed, with such modification we observed a relevant decrease (about 0.3 V) in the oxidation potential due to the electron donating properties of the nitrogen atom. Therefore, Fc-peptides **2** and **4-6**, endowed with redox

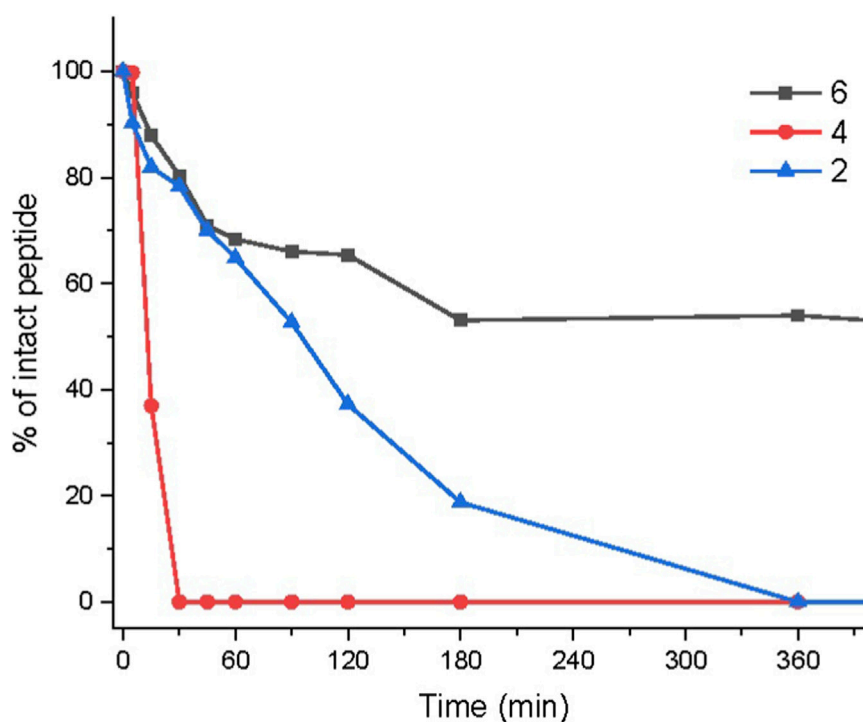


FIGURE 8
Proteolytic degradation in human serum of the peptides **2**, **4** and **6**, represented as the percentage of intact peptide over time calculated as the HPLC-peak area.

values compatible with the intracellular potentials, might result to be good candidates for developing new and effective antitumor agents.

With our new compounds we can also evaluate a possible influence of the spacer on the Fc redox potential. As compared to the effect of the Fc-NH-CO- group, the spacer appears to be of lesser importance, although a small reduction in the redox potential is anyway observed when comparing **1** with **3** and **2** (or **4**) with **5**. As previously stated, such reduction in **3** and **5** (compounds with the longest spacers) is likewise due to the larger separation between Fc and the electron-withdrawing C=O at the end of the spacer. In any case, despite its marginal influence on the Fc oxidation we believe that a spacer should be maintained, as clearly demonstrated by previous work (Zhou et al., 2012).

At variance, a too long spacer may hamper the protection exerted by Fc against the enzymatic degradation of the peptide moieties. Indeed, **4** is rapidly degraded by enzymes, whereas **2** with just one methylene less in the spacer exhibited a slower degradation rate. However, compound **6** characterized by the same spacer of **4** but having a tripeptide instead of a dipeptide regains enzymatic stability. Most probably, this resistance is due to the folded structure (a β -turn) adopted by the tripeptide both in solution (see NMR analysis) and in the crystal state (see X-ray diffraction analysis).

In addition, this folded structure has a moderate effect also on the Fc redox potentials because in a β -turn the amide carbonyls are parallelly aligned (as in the α - and 3_{10} -helix) and oriented with the carbonyl oxygen pointing towards the C-terminus of the peptide. In such a disposition a macrodipole forms, with the partial positive charge located at the N-terminus side of the tripeptide, *i.e.*, close to the Fc unit (Donoli et al., 2011; Biondi et al., 2021; Santi et al., 2022).

Thus, a longer helical peptide, with a higher dipole moment, is expected to decrease even more the $E_{1/2}$ value of Fc.

5 Conclusion

The electrochemical investigation carried out on our newly synthesized Fc-conjugates reveals that the way Fc is connected to the peptide (Fc-NH-CO-) plays the major role in bringing the Fc oxidation potential closer to that of physiological environments. The length of the spacer and of the peptide appears to have an effect as well, but of lesser importance. However, our finding on the influence of a single β -turn suggests that the use of longer, helical peptides will undoubtedly increase the impact on the Fc oxidation, because they generate a larger macrodipole (Donoli et al., 2011; Donoli et al., 2013; Biondi et al., 2021; Santi et al., 2022). Therefore, by combining the nature of the Fc connection with the lengths of spacer and peptide we can better design Fc-constructs able to act as anticancer drugs. Starting from these results, we now plan to move a step forward. We expect to be able to identify lead compounds with potential anticancer activity by designing a second generation of Fc-peptides with the following features: (i) an N-connection to Fc (both Fc-NH-CO- and Fc-NH-CH₂-); (ii) a relatively long spacer; (iii) a helical peptide or a peptide known to interact selectively with receptors over-expressed in cancer cells (Zhou et al., 2012; Ludwig et al., 2021). Since our experiments with human serum suggest that both peptide conformation and Fc itself may protect against enzyme degradation, we hypothesize that even a non-ordered and degradable peptide can be employed if it selectively

guides the compound towards cancer cells. In this case, we may design a conjugate composed by Fc-long spacer-peptide-Fc, the second Fc unit having only the function of protecting the peptide from enzymatic cleavage.

Data availability statement

Cambridge Crystallographic Data Centre (CCDC) numbers 2497229-2497231 contain the supplementary crystallographic data for this paper. These data are provided free of charge by the joint CCDC and Fachinformationszentrum Karlsruhe Access Structures service www.ccdc.cam.ac.uk/structures

Ethics statement

Ethical approval was not required for the studies on humans in accordance with the local legislation and institutional requirements because only commercially available established cell lines were used.

Author contributions

AD: Writing – original draft, Conceptualization, Methodology, Data curation, Investigation. BB: Methodology, Writing – original draft, Investigation, Funding acquisition, Supervision, Conceptualization. AB: Writing – original draft, Data curation, Methodology, Investigation. RC: Writing – review and editing, Methodology, Investigation, Data curation. LL: Methodology, Investigation, Writing - review and editing, Data curation. MŠ: Writing - review and editing, Methodology, Data curation, Investigation. BC: Methodology, Data curation, Investigation, Writing - review and editing. FF: Supervision, Writing - review and editing, Writing - original draft, Conceptualization, Methodology, Investigation, Funding acquisition. MR: Writing - original draft, Investigation, Formal Analysis, Data curation, Methodology. SS: Writing – original draft, Conceptualization, Methodology, Funding acquisition, Writing – review and editing, Supervision.

Funding

The author(s) declared that financial support was received for this work and/or its publication. BB, FF, and SS are grateful to the

Italian Ministry of Research for the financial support through PRIN 2020 NO. 2020833Y75.

Acknowledgements

The Bruker D8 Venture diffractometer at Department of Chemistry of the University of Padova was funded by the MUR-“Dipartimenti di Eccellenza” grantC2.”

Conflict of interest

The author(s) declared that this work was conducted in the absence of any commercial or financial relationships that could be construed as a potential conflict of interest.

Generative AI statement

The author(s) declared that generative AI was not used in the creation of this manuscript.

Any alternative text (alt text) provided alongside figures in this article has been generated by Frontiers with the support of artificial intelligence and reasonable efforts have been made to ensure accuracy, including review by the authors wherever possible. If you identify any issues, please contact us.

Publisher's note

All claims expressed in this article are solely those of the authors and do not necessarily represent those of their affiliated organizations, or those of the publisher, the editors and the reviewers. Any product that may be evaluated in this article, or claim that may be made by its manufacturer, is not guaranteed or endorsed by the publisher.

Supplementary material

The Supplementary Material for this article can be found online at: <https://www.frontiersin.org/articles/10.3389/fchbi.2026.1736812/full#supplementary-material>

References

- Albini, F., Biondi, B., Di Stasi, A., Schivo, A., Mardirossian, M., Scocchi, M., et al. (2025). Fragments of cathelicidins PMAP-36 and BMAP-27 and their D-enantiomers: effects of all D substitutions on structure, protease resistance and antimicrobial properties. *Bioorg. Chem.* 163, 108715. doi:10.1016/j.bioorg.2025.108715
- Amatore, C., Lefrou, C., and Pflüger, F. (1989). On-line compensation of ohmic drop in submicrosecond time resolved cyclic voltammetry at ultramicroelectrodes. *J. Electroanal. Chem.* 270, 43–59. doi:10.1016/0022-0728(89)85027-2
- Bauer, W., Polborn, K., and Beck, W. (1999). Metal complexes of biologically important ligands, CXIV ferrocenyl-oxazolones as N and C donors in Pd(II), Pt(II) and Ir(III) complexes and ferrocenyl-dipeptides. *J. Organomet. Chem.* 579, 269–279. doi:10.1016/S0022-328X(99)00009-1
- Biondi, B., Bisello, A., Cardena, R., Schiesari, R., Cerveson, L., Facci, M., et al. (2021). Flat bis-ferrocenyl end-capped peptides: the influence of the molecular skeleton on redox properties. *ChemElectroChem* 8, 2693–2700. doi:10.1002/celec.202100597
- Biondi, B., Bisello, A., Cardena, R., Schiesari, R., Facci, M., Cerveson, L., et al. (2022). Conformational analysis and through-chain charge propagation in ferrocenyl-conjugated homopeptides of 2,3-Diaminopropionic acid (dap) e202100966. *Eur. J. Inorg. Chem.* 2022, e202100966. doi:10.1002/ejic.202100966
- Bisello, A., Biondi, B., Cardena, R., Schiesari, R., Crisma, M., Formaggio, F., et al. (2023). Modulation of ferrocene-ferrocene interactions by varying their reciprocal positions in α -Dap/Aib helical peptides. *Inorganics* 11, 482. doi:10.3390/inorganics11120482

- Boros, S., Gáspári, Z., and Batta, G. (2018). Accurate NMR determinations of proton-proton distances. *Annu. Rep. NMR Spectrosc.* 94, 1–39. doi:10.1016/bs.armr.2017.12.002
- Chaudhary, A., and Poonia, K. (2024). The redox mechanism of ferrocene and its physicochemical and biochemical compounds in anticancer therapy: a mini review. *Inorg. Chem. Commun.* 134, 109044. doi:10.1016/j.inoche.2021.109044
- Crisma, M., Valle, G., Moretto, V., Formaggio, F., Toniolo, C., and Albericio, F. (1998). Reactive intermediates in peptide synthesis: molecular and crystal structures of HOAt and HOObt, and some ester and amide derivatives of HOBT, HOAt and HOObt. *Lett. Pept. Sci.* 5, 247–258. doi:10.1023/A:1008878209941
- Doi, M., Inoue, M., Tomoo, K., Ishida, T., Ueda, Y., Akagi, M., et al. (1993). Structural characteristics of enantiomeric DNA: crystal analysis of racemates of the d(CGCGCG) duplex. *J. Am. Chem. Soc.* 115, 10432–10433. doi:10.1021/ja00075a098
- Dolomanov, O. V., Bourhis, L. J., Gildea, R. J., Howard, J. A. K., and Puschmann, H. (2009). OLEX2: a complete structure solution, refinement and analysis program. *J. Appl. Cryst.* 42, 339–341. doi:10.1107/S0021889808042726
- Donoli, A., Marcuzzo, V., Moretto, A., Toniolo, C., Cardena, R., Bisello, A., et al. (2011). Charge mapping in 3_{10} -Helical peptide chains by oxidation of the Terminal Ferrocenyl Group. *Org. Lett.* 13, 1282–1285. doi:10.1021/ol102864s
- Donoli, A., Marcuzzo, V., Moretto, A., Crisma, M., Toniolo, C., Cardena, R., et al. (2013). New bis-Ferrocenyl end-capped peptides: synthesis and charge transfer properties. *Biopolymers* 100, 14–24. doi:10.1002/bip.22197
- Gasser, G., Ott, I., and Metzler-Nolte, N. (2011). Organometallic anticancer compounds. *J. Med. Chem.* 13 (54), 3–25. doi:10.1021/jm100020w
- Griesinger, C., Otting, G., Wüthrich, K., and Ernst, R. R. (1988). Clean TOCSY for proton spin system identification in macromolecules. *J. Am. Chem. Soc.* 110, 7870–7872. doi:10.1021/ja00231a044
- Harry, A. G., Butler, W. E., Manton, J. C., Pryce, M. T., O'Donovan, N., Crown, J., et al. (2014). The synthesis, structural characterization and *in vitro* anti-cancer activity of novel 1-alkyl-10-N-para-(ferrocenyl) benzoyl dipeptide esters. *J. Organomet. Chem.* 757, 28–35. doi:10.1016/j.jorganchem.2014.01.031
- Hummel, R.-P., Toniolo, C., and Jung, G. (1987). Conformational transitions between Enantiomeric 3_{10} -Helices. *Angew. Chem. Int. Ed.* 26, 1150–1152.
- Jenssen, H., and Aspö, S. I. (2008). In *Peptide-based drug design: serum stability of peptides*. Editor L. Otvos (Totowa, NJ: Humana Press), 177–186. doi:10.1002/anie.198711501
- Kovacic, P. (2007). Unifying mechanism for anticancer agents involving electron transfer and oxidative stress: clinical implications. *Med. Hypotheses* 69, 510–516. doi:10.1016/j.mehy.2006.08.046
- Kovacic, P., Popp, W. J., Ames, J. R., and Ryan, M. D. (1988). Anti-cancer action of metal complexes: Electrontransfer and oxidative stress? *Chem. Fac. Res. Publ.* 602. Available online at: https://epublications.marquette.edu/chem_fac/602.
- Ludwig, B. S., Tomassi, S., Di Maro, S., Di Leva, F. S., Bengel, A., Reichart, F., et al. (2021). The organometallic ferrocene exhibits amplified anti-tumor activity by targeted delivery via highly selective ligands to $\alpha\beta3$, $\alpha\beta6$, or $\alpha5\beta1$ integrins. *Biomaterials* 271, 120754. doi:10.1016/j.biomaterials.2021.120754
- Meoli, A., Riganti, C., Costamagna, C., Bieganski, P., Kopecka, J., and Kowalsky, K. (2025). Two are better than one: a case study of the biferrrocenyl-thymidine “click” conjugate biFcT as novel ferroptosis-inducing agent in lung cancer cells. *Bioorg. Chem.* 163, 108690. doi:10.1016/j.bioorg.2025.108690
- Mooney, A., Corry, A. J., O'Sullivan, D., Rai, K. D., and Kenny, P. T. M. (2009). The synthesis, structural characterization and *in vitro* anti-cancer activity of novel N-(3-ferrocenyl-2-naphthoyl) dipeptide ethyl esters and novel N-(6-ferrocenyl-2-naphthoyl) dipeptide ethyl esters. *J. Organomet. Chem.* 694, 886–894. doi:10.1016/j.jorganchem.2008.09.064
- Neuse, E. W., and Kanzawa, F. (1990). Evaluation of the activity of some water-soluble ferrocene and ferricenium compounds against carcinoma of the lung by the human tumor clonogenic assay. *Appl. Organomet. Chem.* 4, 19–26. doi:10.1002/aoc.590040105
- Ornelas, C. (2011). Application of ferrocene and its derivatives in cancer research. *New J. Chem.* 35, 1973–1985. doi:10.1039/C1NJ20172G
- Ornelas, C., and Astruc, D. (2023). Ferrocene-Based drugs, delivery nanomaterials and fenton mechanism: state of the art, recent developments and prospects. *Pharmaceutics* 15, 2044. doi:10.3390/pharmaceutics15082044
- Patra, M., and Gasser, G. (2017). The medicinal chemistry of ferrocene and its derivatives. *Nat. Rev. Chem.* 1, 0066. doi:10.1038/s41570-017-0066
- Peggion, C., Schivo, A.; M., Oancea, S., Popovici, L.-F., Călin, T., Mkrtychyan, A., et al. (2025). Synthesis and biological activity of ultrashort antimicrobial peptides bearing a non-coded amino acid. *J. Pept. Sci.* 31, e70021. doi:10.1002/psc.70021
- Rance, M., Sørensen, O. W., Bodenhausen, G., Wagner, G., Ernst, R. R., and Wüthrich, K. (1983). Improved spectral resolution in COSY 1H NMR spectra of proteins via double quantum filtering. *Biochem. Biophys. Res. Commun.* 117, 479–485. doi:10.1016/0006-291X(83)91225-1
- Santi, S., Bisello, A., Cardena, R., Tomelleri, S., Schiesari, R., Biondi, B., et al. (2021). Flat, ferrocenyl-conjugated peptides: a combined electrochemical and spectroscopic study. *ChemPlusChem* 86, 723–730. doi:10.1002/cplu.202100072
- Santi, S., Biondi, B., Cardena, R., Bisello, A., Schiesari, R., Tomelleri, S., et al. (2022). Helical versus flat bis-ferrocenyl end-capped peptides: the influence of the molecular skeleton on redox properties. *Molecules* 27, 6128. doi:10.3390/molecules27186128
- Sheldrick, G. M. (2015). SHELXT – integrated space-group and crystalstructure determination. *Acta Cryst. A* 71, 3–8. doi:10.1107/S2053273314026370
- Toniolo, C., Peggion, C., Crisma, M., Formaggio, F., Shui, X., and Eggleston, D. S. (1994). Structure determination of racemic trichogin A IV using centrosymmetric crystals. *Nat. Struct. Mol. Biol.* 1, 908–914. doi:10.1038/nsb1294-908
- Venkatachalam, C. M. (1968). Stereochemical criteria for polypeptides and proteins. V. Conformation of a system of three linked peptide units. *Biopolymers* 6, 1425–1436. doi:10.1002/bip.1968.360061006
- Wang, T., and Astruc, D. (2025). Electron-reservoir applications of ferrocenes and other late transition-metal sandwich complexes: flow batteries, sensing, catalysis, and biomedicine. *Coord. Chem. Rev.* 524, 16300. doi:10.1016/j.ccr.2024.216300
- Wüthrich, K. (1991). *NMR of proteins and nucleic acids*. Chichester, UK: Wiley.
- Xu, H. G., Annamadov, S., and Mokhir, A. (2022). 4-Ferrocenylaniline-based ROS-responsive prodrugs with anticancer activity. *J. Organomet. Chem.* 964, 122305. doi:10.1016/j.jorganchem.2022.122305
- Zawadke, L. E., and Berg, J. E. (1993). The structure of a centrosymmetric protein crystal. *Prat. Struct. Funct. Genet.* 16, 301–305. doi:10.1002/prot.340160308
- Zhou, B., Li, J., Feng, B., Ouyang, Y., Liu, Y., and Zhou, F. (2012). Syntheses and *in vitro* antitumor activities of ferrocene-conjugated arg-gly-asp peptides. *J. Inorg. Biochem.* 116, 19–25. doi:10.1016/j.jinorgbio.2012.06.014